2007

Role of Leu[superscript B 10] in cytoglobin and comparison of direct and indirect measurements of hexacoordinate hemoglobin ligand affinity

Jordan Richard Witmer
Iowa State University

Role of Leu^{B10} in cytoglobin and comparison of direct and indirect measurements of hexacoordinate hemoglobin ligand affinity

By

Jordan Richard Witmer

A thesis submitted to the graduate faculty

in partial fulfillment of the requirements for the degree of

MASTER OF SCIENCE

Major: Biochemistry

Program of Study Committee:
Mark Hargrove, Major Professor
Michael Shogren-Knaak
Patricia Thiel

Iowa State University

Ames, Iowa

2007

Table of Contents

List of Figures

Abstract

Hexacoordinate hemoglobins (HxHbs) have recently been discovered and have been found in nearly all living organisms. In humans, hxHbs are represented by neuroglobin (Ngb) and cytoglobin (Cgb). While Ngb is principally found in the brain, Cgb is ubiquitously expressed in all tissues. Ligand binding in hexacoordinate hemoglobins is complex due to the reversible coordination of the heme iron by the distal histidine. Hexacoordination regulates ligand binding and is regulated by specific residues in the heme pocket including the B10 position. Therefore, we investigated the influence of Leu^{B10} on hexacoordination and ligand binding in Cgb. Ligand binding was analyzed for recombinant proteins, Cgb B10A Cgb B10F. The results obtained showed that Leu^{B10} plays a crucial in hexacoordination. Interestingly, due to the mutants' low CO affinity it was possible to measure the CO affinity equilibrium constant (K_a) by equilibrium titration similar to the K_a calculated from individual rate constants extracted from kinetics.

Chapter 1: Introduction

Background

Hemoglobins

Hemoglobins are commonly known for their role in oxygen transport. An example is the tetrameric hemoglobin found in red blood cells, and myoglobin found in muscles to temporarily store oxygen until it is needed for aerobic respiration in areas of high energetic needs. However, the hemoglobin family is far more complex than simple oxygen transporters. Hemoglobins have been found in all walks of life including plants, animals and prokaryotes. Hemoglobins are characterized by the coordination of a heme molecule and portraying the globin fold, an arrangement of eight alpha helices named A through H. The heme iron is always found coordinated to the proximal histidine, found in the heme pocket on the side opposite to the site of ligand binding. The iron within the heme is coordinated to four nitrogens, all in one plane, in addition to the proximal histidine. These five coordinating sites to the heme iron are termed pentacoordination. The heme iron can exist in two oxidation states: ferric, Fe^{3+}, and ferrous, Fe^{2+}. The roles of the majority of hemoglobins remains unclear with many possible functions including: oxygen storage, transport and scavenging, detoxification of nitric oxide, sensing of oxygen and other small heme ligands (Kundu *et al* 2003), protection during hypoxia (Trent et al 2002) and signal transduction (Wakasugi *et al* 2003).

Hexacoordination

Many of the hemoglobins found throughout a variety of organisms exhibit internal hexacoordination, when the heme iron is coordinated to distal histidine as well as the proximal histidine. Other hemoglobins that only have the proximal histidine bound to the heme iron are classified as pentacoordinate. Despite the binding of the distal histidine to the last available site for ligands to bind, hexacoordinate hemoglobins are still capable of binding a variety of ligands with high affinity. The difference between pentacoordination and hexacoordination can be observed in the figure below.

Figure 1

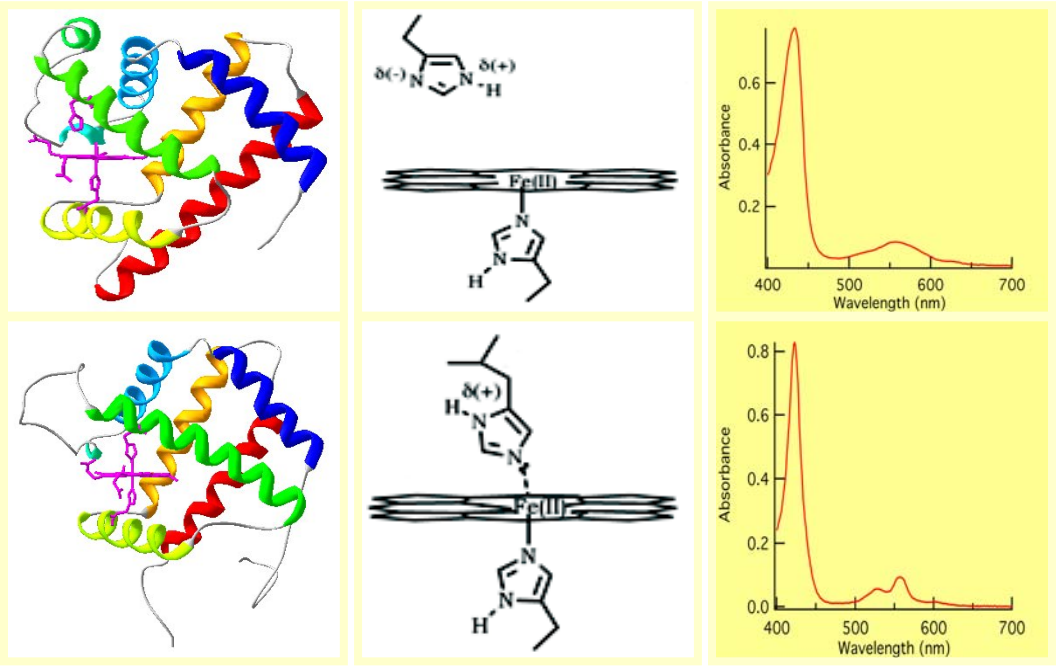

Fig 1. An example of pentacoordination depicted in the top half (Brucker *et al* 1996) and hexacoordination in the lower half (Hargrove *et al* 2000B). The left side shows a three-dimensional representation of the crystal structure of the protein, the middle illustrates the coordination the histidines to the heme iron in the ferrous state and the right side displays an absorbance spectrum of the species.

Cytoglobin

Cgb is a hexacoordinate hemoglobin which is expressed ubiquitously in human tissues and was discovered five years ago, shortly after the discovery of neuroglobin, another mammalian hexacoordinate hemoglobin. Cgb is thought to play a role in protection during hypoxia and scavenge reactive molecules such as nitric oxide because it is expressed in most tissues and is not found in high enough concentrations to adequately transport or store oxygen.

Justification of This Research

Cgb is the only known hexacoordinate hemoglobin to have a leucine at the B10 position, B10 refers to the 10^{th} residue on the B helix. Plant hexacoordinate hemoglobins predominantly contain phenylalanine at the B10 site and a tyrosine can be found in most of the other known hexacoordinate hemoglobins. Pentacoordinate hemoglobins commonly possess a leucine at B10 position similar to Cgb. Even though Cgb possess a common pentacoordinate heme pocket residue, it still maintains its hexacoordinate arrangement (Fig 2).

Figure 2

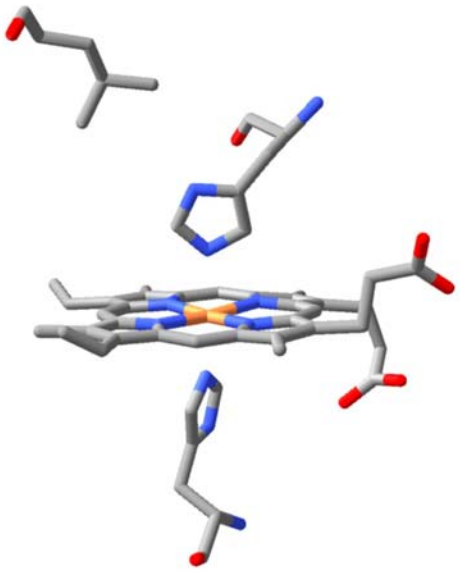

Fig 2. A depiction of the relative proximity of the Leucine^{B10} to the distal histidine in cytoglobin (DeSanctis *et al* 2004)

Myoglobin's B10 residue has been well characterized and is known to be responsible for stabilizing the distal histidine, which allows it to form a hydrogen bond with bound oxygen (Carver *et al* 1992). Likewise, in leghemoglobin, a plant oxygen scavenging protein, the B10 residue influences the distal histidine in its stabilization of bound ligands (Kundu *et al* 2003B). The role B10 in hexacoordinate hemoglobins found in plants is to destabilize the distal histidine from coordinating too tightly to the heme iron (Smagghe *et al* 2006B). The B10 site in hemoglobins has proven to be a key element in regulating the distal heme pocket that attributes to the characteristics of the proteins allowing them to function properly. By altering the B10 position in hemoglobins, the mechanism by which this key residue regulates the distal heme pocket can be studied.

A primary sequence alignment was done using Kalign (Lassman *et al* 2005) for a plant symbiotic pentacoordinate hemoglobin (Lba), a mammalian pentacoordinate hemoglobin (Mb), two mammalian hexacoordinate hemoglobins (Cgb and Ngb), a plant non-symbiotic hexacoordinate hemoglobin, a non-vertebrate hexacoordinate hemoglobin (Ascaris Hb) and prokaryotic hexacoordinate hemoglobin (HbN).

Figure 3

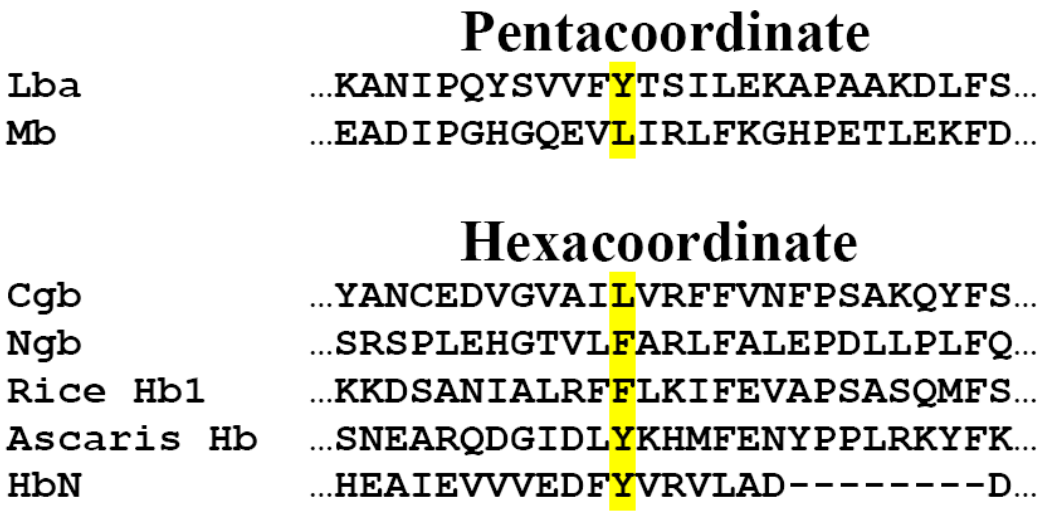

Fig 3. Alignment of initial residues surrounding the B10 site. (Lba – soybean legume, Mb – Myoglobin, Cgb – Cytoglobin, Ngb – Neuroglobin, Ascaris {Nematode} Hb, HbN – Tuberculosis).

The mutations made for Cgb were B10A and B10F in order to characterize the mutants of smaller and larger residues and compare to the wild type to better understand the role of Leu^{B10}.

Approach

Despite the competition exogenous ligands have with the distal histidine for hexacoordinate hemoglobins, ligands still have a high affinity for the protein making it difficult and nearly impossible to measure ligand affinity directly because of stoichiometric binding of the ligand. Hexacoordinate hemoglobins have two equilibriums to transcend in order to bind an exogenous ligand: the reversible coordination of the distal histidine and the binding of the ligand itself. Eq. 1 demonstrates the three states hexacoordinate hemoglobins can exist when an exogenous ligand is present (Hargrove 2000A).

Equation 1

$$Hb_H \underset{k_H}{\overset{k_{-H}}{\Leftrightarrow}} Hb_P + L \underset{k_L}{\overset{k'_L}{\Leftrightarrow}} Hb_L$$

As a result of the reversibly coordinating histidine, a more complicated mathematical model describes the affinity of exogenous ligands for the protein. An expression for affinity constants representing this reaction scheme is derived below (Watts 1999).

Equation 2: The simple binding of a ligand to pentacoordinate hemoglobin

$$Hb_P + L \underset{k_L}{\overset{k'_L}{\Leftrightarrow}} Hb_L$$

Equation 3: The equilibrium affinity of ligand bound to pentacoordinate hemoglobin

$$Ka,_P = \frac{[Hb_L]}{[Hb_P][L]}$$

Equation 4: Set the concentration of Hb_L equal to 1

$$[Hb_L] = Ka,_P[L]$$

Equation 5: Fraction of ligand bound for pentacoordinate hemoglobin

$$fHb_L = \frac{[Hb_L]}{[Hb_L] + [Hb_P]}$$

Equation 6: Set the amount of $[Hb_P]$ equal to 1

$$fHb_L = \frac{[Hb_L]}{[Hb_L] + 1}$$

Equation 7: Substitute Eq. 4 into Eq. 6

$$\left[fHb_L = \frac{Ka,_P[L]}{1 + Ka,_P[L]} \right]$$

Equation 8: Equilibrium of hexacoordination from Eq. 1

$$K_H = \frac{[Hb_H]}{[Hb_P]}$$

Equation 9: Eq. 8 rearranged and set the concentration of Hb_H equal to 1

$$[Hb_P] = \frac{1}{K_H}$$

Equation 10: Substitute Eq. 9 into Eq. 3 and solve for Hb_L

$$[Hb_L] = \frac{Ka,_P[L]}{K_H}$$

Equation 11: Fraction of ligand bound for hexacoordinate hemoglobin

$$fHb_L = \frac{[Hb_L]}{[Hb_H] + [Hb_P] + [Hb_L]}$$

Equation 12: Substitute Eq. 10 and Eq. 9 into Eq. 11

$$fHb_L = \frac{\frac{Ka,_P[L]}{K_H}}{1 + \frac{1}{K_H} + \frac{Ka,_P[L]}{K_H}}$$

Equation 13: Multiply right side of Eq. 12 by 1, (K_H/K_H)

$$fHb_L = \frac{Ka,_P[L]}{K_H + 1 + Ka,_P[L]}$$

Equation 14: Multiply right side of Eq. 13 by 1, ($1/K_H$ / $1/K_H$)

$$\left[fHb_{L,\,H} = \frac{\left(\frac{Ka,_P}{1+K_H}\right)[L]}{1+\left(\frac{Ka,_P}{1+K_H}\right)[L]} = \frac{Ka,_H[L]}{1+Ka,_H[L]} \right]$$

Equation 15: By analogy to Eq. 7, the equilibrium affinity of for ligand is shown in Eq. 17

$$\left[fHb_{L,\,H} = \frac{\left(\frac{Ka,_P}{1+K_H}\right)[L]}{1+\left(\frac{Ka,_P}{1+K_H}\right)[L]} = \frac{Ka,_H[L]}{1+Ka,_H[L]} \right]$$

Equation 16: The equilibrium for ligand affinity for hexacoordinate hemoglobins is described below

$$\left[Ka,_H = \frac{Ka,_P}{1+K_H} \right]$$

Therefore, by kinetically measuring the association and dissociation rates for the distal histidine and ligand, one can calculate the affinity of the ligand for the hexacoordinate protein.

Flash Photolysis

The rate at which the ligand binds to the pentacoordinate form of the hemoglobin can be around a nanosecond timescale. Flash photolysis allows for the observation of such rates by photolysing the protein-ligand bound complex long enough for the ligand to escape from the matrix of the protein. Once the light pulse is turned off, the ligand essentially binds to the pentacoordinate form of the hemoglobin making it possible to measure the

association rate of the ligand assuming a pseudo first order reaction. The equation shown below describes the plot of the observed rate from flash photolysis (Hargrove 2000A).

Equation 17:

$k_{obs} = k_{-H} + k_H + k'_L[L]$

The slope of the plot yields the rate constant of the association rate of ligand while the y-intercept equals the sum of the association and dissociation rate of the distal histidine.

Rapid Mixing

Rapid mixing of the hexacoordinate hemoglobin and differing concentrations of ligand allow for the measuring of the dissociation rate of the distal histidine when the ligand concentrations are high enough to cause it to be the rate limiting step. The observed rate of ligand binding to the hexacoordinate hemoglobins assuming a steady state for the pentacoordinate form for the unbound protein is described in Eq. 18.

Equation 18:

$$k_{obs} = \frac{(k_{-H})(k'_{CO})[CO]}{k_H + k_{-H} + k'_{CO}[CO]}$$

CO Dissociation

CO dissociation can be measured by mixing CO-bound protein with a high concentration of NO. The dissociation rate was calculated assuming a pseudo first order reaction CO dissociation is rate limiting and the irreversible binding of the NO to the protein. The

signal resulting from CO dissociating can be fit to a nexponential to extract the rate of dissociating ligand (Olson 1981).

CO Equilibrium Titration

Interestingly enough, it was possible to measure the CO affinity for the mutant proteins by CO equilibrium titration. A K_a can be measured by fitting the fraction bound vs CO concentration while considering the concentration of protein in Eq. 19.

Equation 19:

$$F_B = \frac{\left(1 + \frac{1}{K_a[P]} + \frac{[L]}{[P]}\right) - \sqrt{\left(1 + \frac{1}{K_a[P]} + \frac{1[L]}{[P]}\right)^2 - 4\frac{[L]}{[P]}}}{2}$$

Electrochemistry

Measuring the midpoint redox potential of hexacoordinate hemoglobins determines the free energy required to reduce the ferric form to the ferrous oxidation state. Midpoint potentials of pentacoordinate hemoglobins have slightly positive values with respect to a standard hydrogen electrode (Smagghe *et al* 2006B). However, hexacoordinate hemoglobins have negative a midpoint potential, demonstrating the ferrous state of pentacoordinate proteins are more thermodynamically stable than their hexacoordinate counterparts. Many factors can affect the midpoint potential of these proteins, but the dominating factor appears to be in the difference of the affinity of the histidine coordinating to the heme iron for the ferric and ferrous states.

Equation 20:

$$\left(\frac{1+K_{H3}}{1+K_{H2}}\right) = e^{-(nF(Eobs-Emid)/RT)}$$

The dependence of the distal histidine's affinity for either oxidation state can be depicted in Eq. 19 (Halder *et al* 2007). This equation illustrates that proteins with a positive midpoint potential have a stronger affinity for the distal histidine in the ferrous state than the ferric state and, inversely, a negative midpoint potential results from stronger affinity for the distal histidine in the ferric state than the ferrous state.

Azide Equilibrium Titration

To further understand the affinity of the distal histidine in the ferric state, azide equilibrium titration can be measured with the understanding that if the affinity of the histidine in the ferric state increases, the overall affinity of the ligand should decrease assuming the ligand affinity in the pentacoordinate form remains constant (Equation 15).

Chapter 2: Results

Flash Photolysis

The association rate constant for CO (k'_{CO}) was found for Cgb Wt, Cgb B10A and Cgb B10F by plotting the observed rates from 100μM, 200μM, 400μM, 600μm, 800μM and 1000μM CO concentrations versus the concentration of CO from flash photolysis. Figure 4 shows these data along with exponential fits to the following equation.

Equation 21:

$$A_t = \Delta A e^{-kt}$$

In this equation, A is the absorbance value at time "t", ΔA is the time course amplitude, and k is the observed rate constant plotted in Figure 4D for each protein. As these reactions are pseudo first order in CO, the bimolecular rate constants are obtained from a plot of k_{obs} versus [CO] (Figure 4D). The computed k'_{CO} from the slope of each of the plots were Cgb Wt ($5.6\mu M^{-1}s^{-1}$), Cgb B10A ($3.7\mu M^{-1}s^{-1}$) and Cgb B10F ($1.8\mu M^{-1}s^{-1}$).

Figure 4

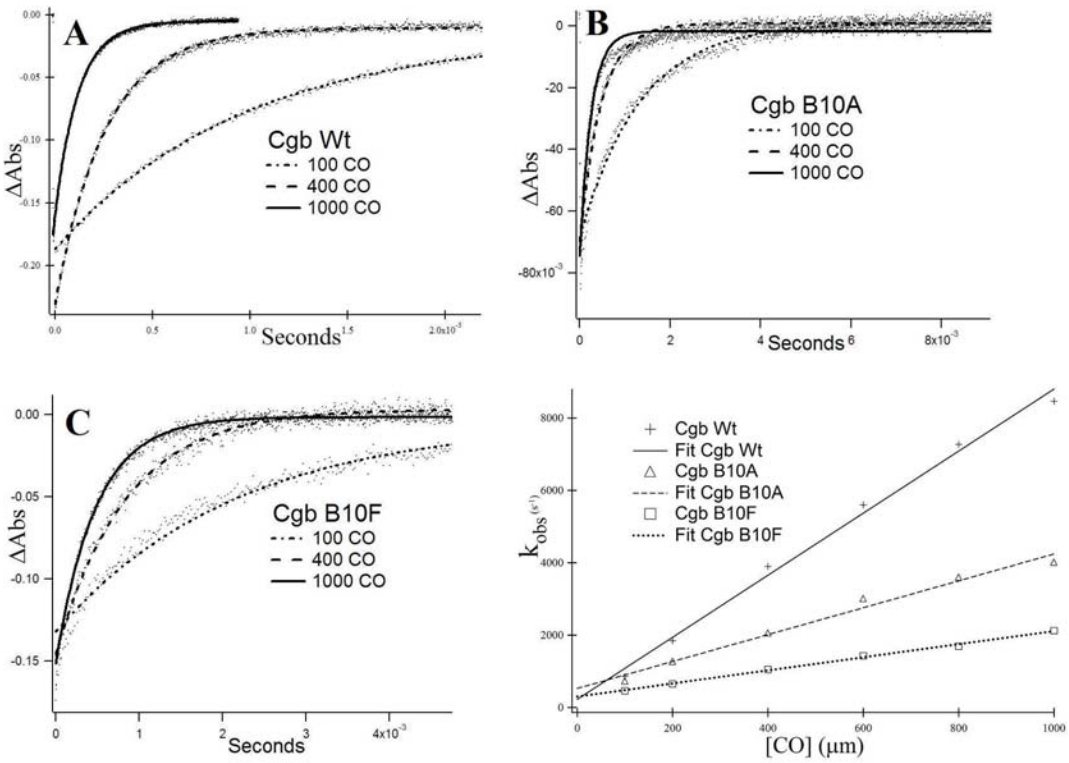

A second run of flash photolysis data were collected in order to better ascertain the association rate of the distal histidine, k_H. The need to collect a second set of data for flash photolysis became apparent after analysis of rapid mixing experiments. Rapid mixing demonstrated that the dissociation rate of the distal histidine, k_{-H}, was to slow to be able to extract k_H. Now knowing that the value of k_{-H} was small enough to assume the y-intercept of the resulting plot of kobs against CO concentration to be equal to k_H when considering Eq. 16 (Hargrove 2000A), data at lower concentrations of CO needed to be collected to better determine the y-intercept. The concentrations of CO used were 10μM to 25μM. The distal histidine association rate was calculated by fitting a line to the data

obtained at lower CO concentrations. The following rates for Cgb Wt, Cgb B10A and Cgb B10F were 250 s^{-1}, 250 s^{-1} and 150s^{-1}.

Rapid Mixing

The observed rate of CO binding as measured by rapid mixing was independent of CO concentration for all three proteins. The k_{-H} was too slow for rapid mixing to be of any use in extracting k_H and k'_{CO} from the plot of the rate observed versus CO concentration (Smagghe *et al* 2006A). Therefore, it was necessary to repeat flash photolysis and measurement of binding rates at low CO concentration to obtain the k_H for each protein.

The data from the wild type protein best fit a double exponential. The initial rate or faster rate was taken to be the rate for k_{-H} which composed about 60% of the change in signal. This data is consistent with the values for Cgb Wt produced from Smagghe et al 2006A.

Figure 5

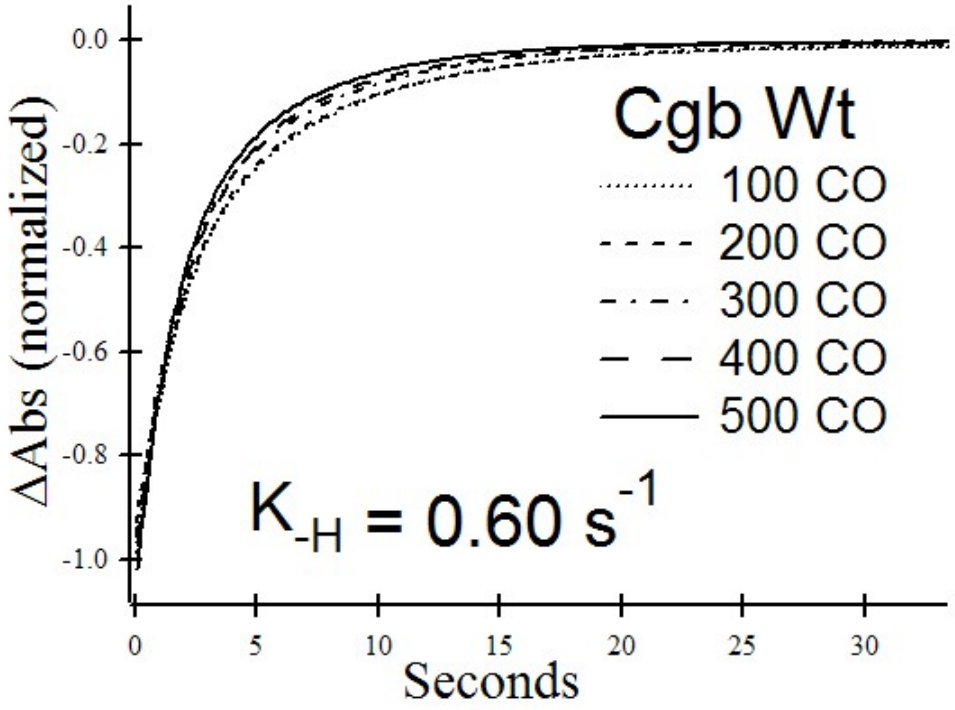

The observed rates for rapid mixing of Cgb B10A were fit to a double exponential. Again, he initial rate was taken to be the rate for k_{-H} which composed about 67% of the change in signal. The rates obtained with concentrations of CO 200μM or less were not used to determine the k_{-H} because there was a loss in amplitude of the signal due to its low CO affinity.

When the data for Cgb B10A was first analyzed, it was believed that it should be fit to the model described in Smagghe et al 2006A for hexacoordinate proteins that exist partially in the pentacoordinate state. This was considered because there was a slight loss in amplitude of the trace obtained for low CO concentrations. The model is used to fit hexacoordinate proteins with a low K_H, such as rice nonsymbiotic hemoglobin (Smagghe

et al 2006A) After further investigation, the small loss of amplitude was due to the protein's low CO affinity. There was no loss of signal, which was originally believed, but a smaller change in amplitude because the protein was not completely bound to CO. The data obtained from rapid mixing with CO concentrations of 200μM or less was not used to derive the k_{-H} for Cgb B10A because the binding of CO was incomplete.

Figure 6

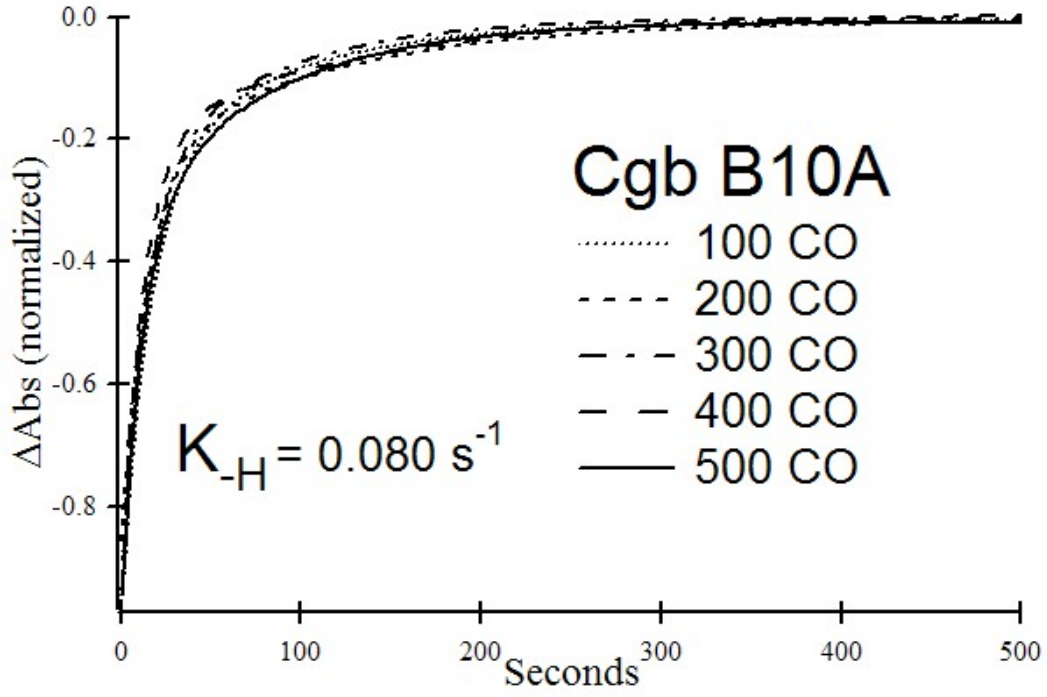

The rapid mixing of Cgb B10F produced rates that were certainly independent of CO concentrations. The data was fitted to a double exponential with the primary rate

composing roughly 76% of the change in amplitude and the rates for CO concentrations of 300 and higher were averaged to calculate k_{-H}.

Figure 7

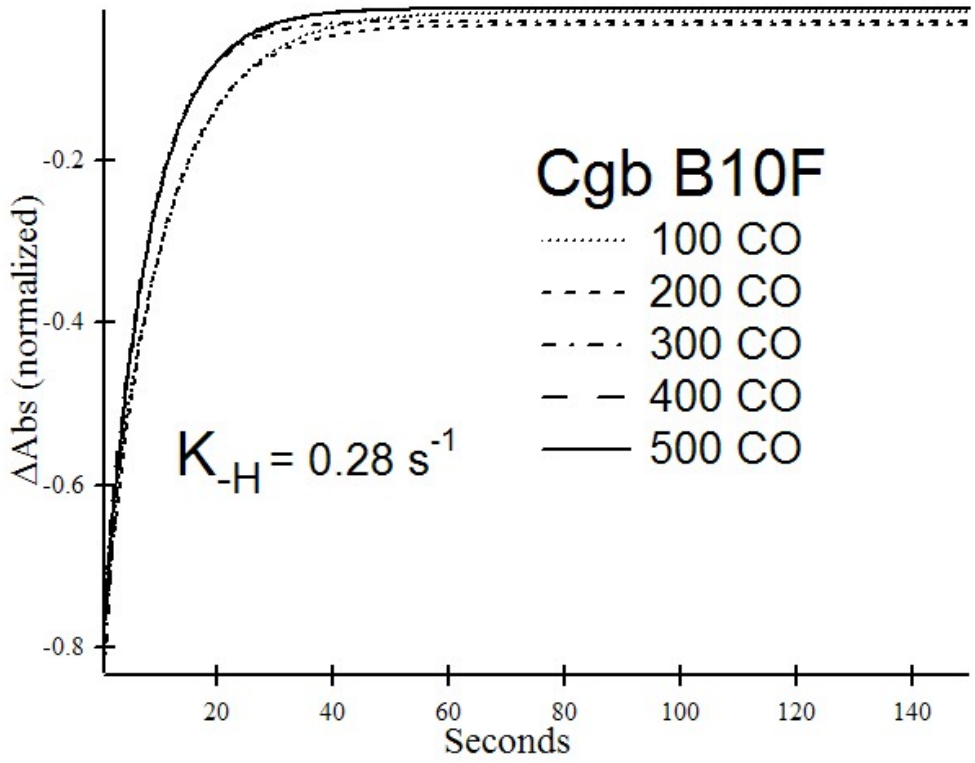

CO Dissociation

The data acquired from CO dissociation experiments were fit to a double exponential curve and the rate was taken to be the dissociation rate of CO, k_{CO}. The faster was taken as the dissociation rate. The rates for Cgb Wt, Cgb B10A, Cgb B10F and Rice Hb1 were $0.0048s^{-1}$, $0.0011s^{-1}$, $0.0080s^{-1}$ and $0.12s^{-1}$.

Figure 8

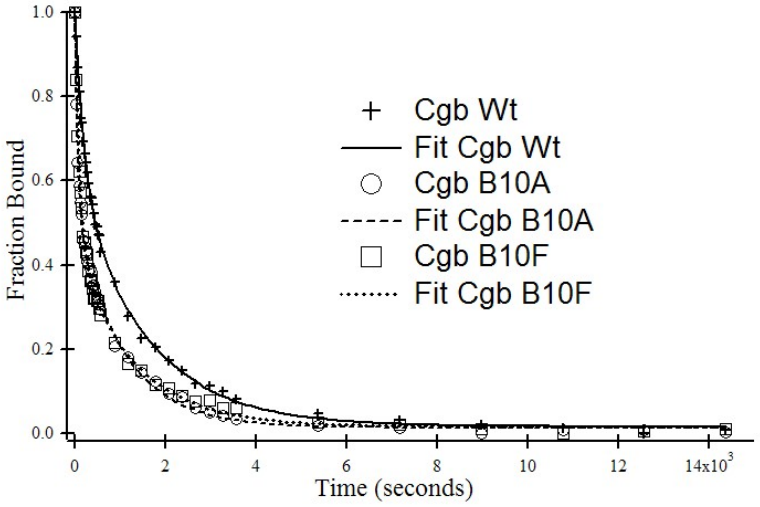

Figure 9

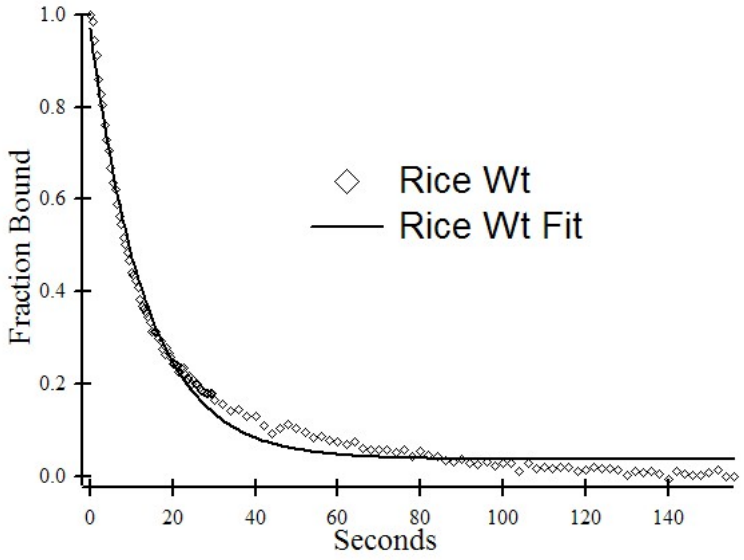

CO Equilibrium Titration

The CO equilibrium association affinity constants obtained by CO equilibrium titration for Cgb Wt, Cgb B10A and Cgb B10F were 3.3μM^{-1}, 0.10μM^{-1} and 0.36μM^{-1}.

Surprisingly, the CO affinity for Cgb B10A and Cgb B10F was low enough to be directly measured by CO equilibrium titration. This was of particular interest because no other hemoglobin has been directly measured for CO affinity. Normally, hemoglobins exhibit stoichiometric binding when equilibrium titrated with CO. To illustrate stoichiometric binding rice nonsymbiotic hemoglobin was used as a positive control. Cgb Wt stoichiometrically binds CO but it appears more drastic in rice.

The fact that we could directly measure CO affinity in these Cgb mutant proteins provided the opportunity for comparison of equilibrium affinity constants measured directly to those calculated from kinetic rate constants using Eq. 16. To make sure we could distinguish between stoichiometric binding and equilibrium binding, another hexacoordinate hemoglobin, Rice nonsymbiotic hemoglobin, was equilibrium titrated to illustrate the problem in directly measuring ligand affinity for hexacoordinate hemoglobins.

Figure 10

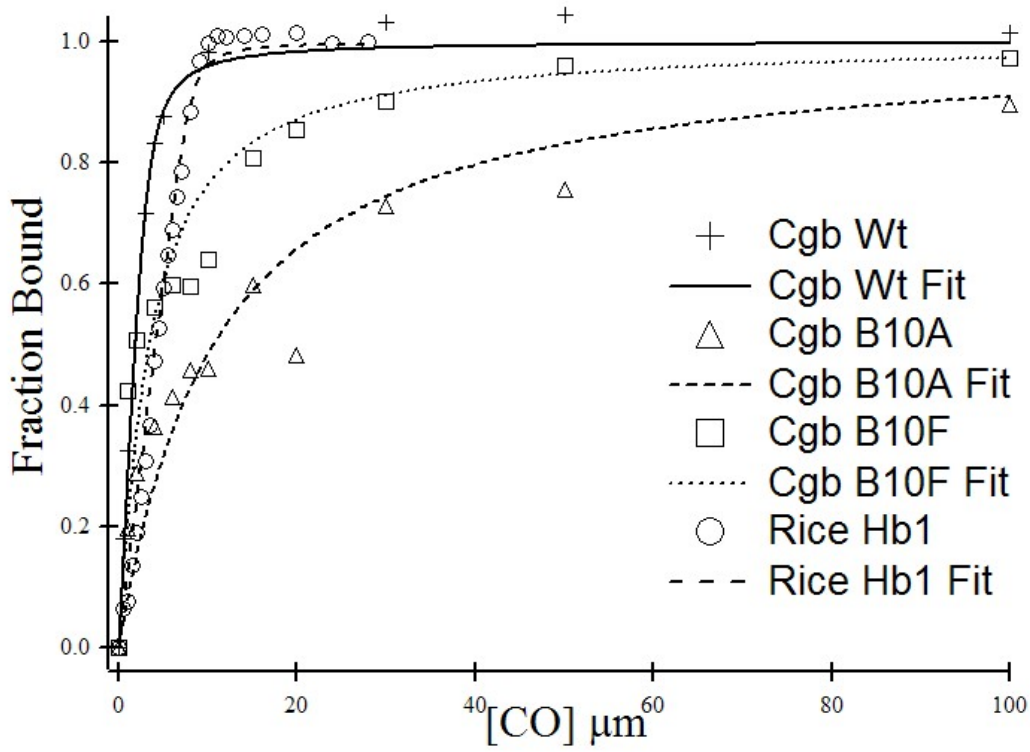

Electrochemistry

Midpoint potentials were extracted from the change in signal due to the oxidation state of the heme iron against the reduction potential by fitting to the following equation (Halder *et al* 2007).

Equation 22:

$$F_{reduced} = \frac{e^{-\left(\frac{nF\ (\ Eobs\ ,-\ Emid\ )}{RT}\right)}}{1+e^{-\left(\frac{nF\ (\ Eobs\ ,-\ Emid\ )}{RT}\right)}}$$

The change in the absorption was measured at 560nm for both proteins and the midpoint potentials extracted from Eq. 22 for Cgb B10A and Cgb B10F were –108mv and –75mV.

Figure 11

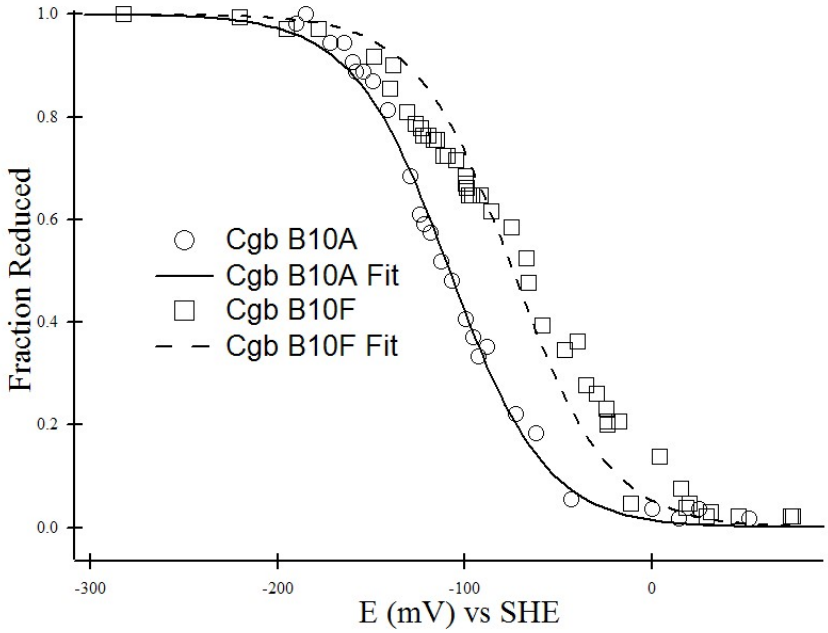

Azide Equilibrium Titration

Azide equilibrium titration studies were done similarly to CO equilibrium titration studies. The change in signal was due to the binding of ligand was fitted to Eq. 19. Azide affinity of Cgb Wt, Cgb B10A, Cgb B10F were $0.12\mu M^{-1}$, $0.055\mu M^{-1}$ and $0.76\mu M^{-1}$.

Figure 12

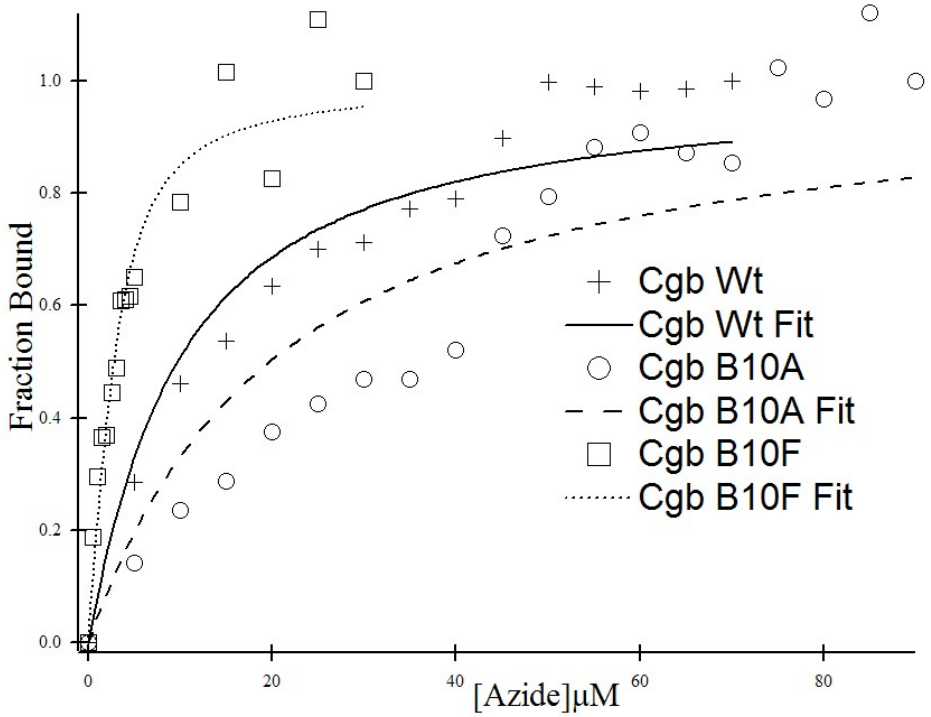

All of the data attained above is shown in Table 1 as well as data from Smagghe *et el* 2006A and Goodman *et al* 2001. The indirectly calculated K_{CO} was found using Eq. 16.

Table 1

Protein	k_H (s^{-1})	k_{-H} (s^{-1})	K_H	$k'_{CO,p}$ ($\mu M^{-1}s^{-1}$)	$k_{CO,p}$ (s^{-1})	$K_{CO,p}$	K_{CO} Indirectly Found (μM^{-1})	K_{CO} Directly Found (μM^{-1})	E_{mid} (mV)	K_{Azide} (μM^{-1})
Cgb Wt	250	0.60	417	8.6	0.0048	1800	4.3	3.3	-28[†]	0.12
Cgb B10A	250	0.080	7100	3.7	0.011	340	0.11	0.10	-110	0.055
Cgb B10F	150	0.28	1200	1.8	0.0080	225	0.42	0.36	-74	0.76
Rice Hb1	75[#]	40[#]	1.9	6.0[*]	0.12	50	17	Tight	n.d.	n.d.

[#]Taken from Smagghe *et al* 2006A, [*]From Goodman *et al* 2001, [†]From Halder *et al* 2007

Chapter 3: Discussion

The importance of the B10 position in hemoglobins has been well characterized. The B10 position in hemoglobins can play a role in the electrostatic environment where ligands bind, influencing the distal histidine position, sterically hindering the ligand and maintaining the overall structure of the heme pocket (Kundu *et al* 2004, Wiltrout *et al* 2005, Adachi *et al* 1992). The role of leucine^{B10} in Cgb appears to be primarily the destabilization of the distal histidine in the ferric and ferrous forms while other functions may exist were not apparent in this study.

Accurately and Indirectly Measuring Ligand Affinity

Due to the dramatic decrease in CO affinity from the substitutions made at the B10 position, it was possible to compare the methods of directly and indirectly obtaining ligand affinity for hexacoordinate hemoglobins. This has never been done before and the results above support the accuracy of indirectly measuring ligand affinity by kinetically extracting the rates required to calculate the association and dissociation rates of the distal histidine and for the ligand in the pentacoordinate state. Previously, all other hexacoordinate hemoglobins exhibit stoichiometric binding of CO, which can be observed in Cgb Wt and Rice Hb1 in figure 10. Stoichiometic binding of ligand occurs when all of the ligand titrated into the mixture binds with the protein. This results in a linear relationship to ligand concentration and the fraction bound until all of the protein is bound. Therefore, no information can be obtained for the ligand affinity from

equilibrium titrations when stoichiometric binding results. Fortunately, the Cgb B10A and Cgb B10F do not exhibit stoichiometric binding of CO as shown in figure 10. Much more of the protein remains unbound to ligand when the ligand is added to the mixture compared with other hexacoordinate proteins and it was possible to visualize the equilibrium instead of assuming all available ligand is bound. The comparison of CO affinity from the indirect method and direct measurement for Cgb B10A (0.11 μM^{-1} vs 0.10μM^{-1}) and Cgb B10F (0.42μM^{-1} vs 0.36μM^{-1}) are well within reason and the unreliability of extracted ligand affinity from ligand titrations becomes apparent when comparing the CO affinities between the methods for Cgb Wt (4.3μM^{-1} vs 3.3μM^{-1}) and Rice Hb1 (17μM^{-1} vs 110μM^{-1}). The accurateness of measuring four kinetic rates from experiments, the models used to describe them, and the model that describes ligand affinity of hexacoordinate hemoglobins appears to be acceptable and true.

Histidine Affinity in the Ferric and Ferrous States

Both of the B10 mutants midpoint potentials decreased compared to the wild type. Therefore, the affinity of the distal histidine for the ferrous state increased more relative to the affinity of the distal histidine for the ferric state. A simpler way of conceiving the change in distal histidine affinity is that (K_{H2}/K_{H3}) increased as a result of the substitutions made at the B10 position. With K_{H2} being known from flash photolysis and rapid mixing, the qualitative changes of K_{H3} could be inferred from the changes in midpoint potentials. Again, both Cgb B10A and Cgb B10F showed an increase in K_{H2} compared to Cgb Wt implicating a greater increase in the K_{H3} for both mutants.

To test this hypothesis, the affinity for an exogenous ligand for the proteins in the ferric state was determined. Considering Eq. 15, an increase in the affinity of the distal histidine will lower the affinity of the ligand for $Ka,_H$ assuming there are trivial changes in $Ka,_P$(Smagghe *et al* 2006). The affinity for azide was obtained for all three proteins in the ferric state. Cgb B10A proved to have lower affinity than Cgb wild type for azide but not as drastic as previously believed and Cgb B10F was found to have a higher affinity refuting the previous prediction of a decreased ligand affinity for the mutants in the ferric state. It is possible that the $K_{azide,P}$ decreased more dramatically than the increase in K_{H3} for the mutants. The change in absorption due to the azide binding was relatively small, a five percent change in the signal, and the Soret peak, the primary absorbance peak in hemoglobins, shifted one nanometer. This in combination of measuring small shifts within the 5 percent change of signal did provide imperfect data. However, Fig. 12 qualitatively demonstrates that K_{azide} for Cgb B10F in the ferric state is higher than the K_{azide} of Cgb Wt. To further investigate the affinity of the distal histidine in ferric and ferrous states, a different ligand, such as cyanide or nitric oxide, could be used to observe its affinity for the ferric protein.

Role of Leucine^{B10}

The substitution of alanine and phenylalanine for leucine at the B10 position, overall, had the same affect. The rates $k_{CO,p}$ and $k'_{CO,p}$ were decreased and k_{-H} was increased as a result of the mutations made. The dissociation rate of the distal histidine decreased considerably for both, by at least a factor of ten, thus increasing the affinity of the distal histidine to the heme iron. The affinity for CO in the pentacoordinate form was greatly

reduced by an increase in $k_{CO,p}$ and a decrease in the $k'_{CO,p}$. Cgb B10F decreased the k_H by half most likely due to the steric hindrance of a larger residue keeping the histidine off the heme iron in the ferrous state. Interestingly, the K_H for CgbB10F increased because of large decrease in the k_{-H}. A larger residue so close to the distal histidine is likely to bump the histidine of the heme iron. This was certainly not the case for Cgb B10F.

Nature's rationale for placing a leucine at the B10 position for Cgb appears to be due to the affinity of distal histidine to the heme iron. Cgb B10A frees up space in the heme pocket while Cgb B10F would fill in much of the available space yet both mutations increase the K_{H2} and K_{H3} immensely. Leucine^{B10} is necessarily playing a vital role in destabilizing the distal histidine in order for the wild type protein to function properly. Similar findings were shown in plant hexacoordinate hemoglobins (Smagghe *et al* 2006B) where mutations of the B10 position increased both K_{H2} and K_{H3}.

In myoglobin, leucine^{B10} is thought to aid in structural stability of the hydrophobic cluster on the distal side of the heme pocket. In the work done by Adachi *et al* 1992, changes in the B10 residue were believed to alter interactions within distal hydrophobic cluster, thus changing the heme pocket structure and ligand binding properties. The mutations made in myoglobin B10 were found to lower the CO association rate. This corresponds with the decrease of CO association rate in the pentacoordinate form due to changing leucine^{B10} to alanine or phenylalanine in Cgb suggesting leucine^{B10}'s importance in the distal heme pocket's organization.

The results demonstrated here indicate that leucine^{B10} in Cgb regulates the affinity of the distal histidine in both ferric and ferrous states of the protein and assists in maintaining the native structural integrity of the distal heme pocket.

Future Studies

For further investigation, structural information for Cgb B10A and Cgb B10F would illuminate the structural changes within the heme pocket. Changes for K_{H3} among Cgb Wt, B10A and B10F need to be elucidated to further comprehend the extent at which leucine^{B10} regulates the distal histidine in the ferric state. The midpoint potentials of Cgb B10A and Cgb B10F relative to Cgb Wt suggest that leucine^{B10} is significantly destabilizing the distal histidine's binding to the heme iron. The affinity for azide in the pentacoordinate form and ferric state of Cgb B10F compared to Cgb Wt may be changing on a scale greater than 1,000 fold. The understanding of these changes in the ferric state may point to the physiological function of Cgb and will help eliminate some of its possible functions. Cgb and myoglobin have similar oxygen affinities and perhaps Cgb serves as an oxygen transporter were myoglobin is not expressed (Trent *et al* 2002). The affects of the mutations will have on the association and dissociation rate of oxygen will give further insight of the possible physiological function of oxygen transport. Hexacoordinate hemoglobins are capable of dioxygenating NO (Perazzolli *et al* 2004). The characterization of the alterations in the B10 site have on detoxifying NO needs to be done in order to narrow down the role of Cgb.

Chapter 4: Methods

Protein Expression and Purification

Cytoglobin cDNA was cloned into the expression vector pET28a and mutants B10A and B10F were made via PCR mutagenesis. All proteins were expressed using the host strain BL21 Star DE3 (Invitrogen) except for Cgb B10F, which was expressed by the host strain C41 (Avidis). Each expression vector was grown in 20 L of Terrific Broth media at 37^0C for 18 hours with 50μg/mL kanamycin sulfate for selection purposes and 1g/L of lactose to auto-induce expression. Cells were harvested by centrifugation using the JA-10 rotor in an Avanti J-E Beckman Coulter centrifuge at 6,000 rpm for 6 minutes to pellet the cells. The pelleted cells were then resuspended in a minimal volume of 50mM sodium phosphate buffer at pH 7.0. The cells were then lysed by passing through an EmulsiFlex-C5 High Pressure Homogenizer at 10,000 psi four times. Lysate was then centrifuged using the JA-14 rotor at 14,000 rpm for ten minutes keeping the supernatant. Ammonium sulfate fractionation was performed at 30%, saving supernatant, and then at 80%, saving the pellet. The pellet was then resuspended and dialyzed into 50mM sodium phosphate buffer pH 7.0. The sample was loaded onto an IMAC Talon His-tag cobalt resin and a 50mM sodium phosphate, 300mM sodium chloride pH 7.0 was washed over the column until the flowthrough reached a 280nm absorbance less than 0.01. The protein was then eluted using the previous buffer with 100mM imidazole added. Fractions were checked using a Varian Cary-Bio Spectrophotometer. The ratio of the 420nm soret peak to the 280nm peak was compared and fractions at a ratio of 2.5 or better were used for experimentation. Fractions below were ran over a Sephacryl S-100

size exclusion column and fractions at a ratio of 2.5 or better were kept. All purified proteins were oxidized to the ferric state before experimentation by adding a slight excess of ferricyanide and then ran over a G25 column to separate the protein from the oxidative reagent.

Flash Photolysis

Flash photolysis experiments were carried out using a 10 Hz Continuum Surelite I YAG laser which photodissociated the ligand by a 5ns pulse at 532nm. The change in absorbance was monitored with a 1P23 photomultiplier tube in combination attached to a manual holographic monochromater. The voltage was read by digital oscilloscope that was triggered electronically by the laser. The light source was provided by a 75-W xenon lamp with a broad band interference filter to remove all light except in the range from 410nm to 440nm. Samples were prepared with 100mM potassium phosphate, pH 7.0, buffer that was bubbled with either CO or N_2 for twenty minutes. Dry sodium dithionite was then added to the solution to concentration of about 200μM. Varying concentrations of CO were made by mixing proper amounts of CO and N2 to produce the desired concentrations of CO needed. The different concentrations of CO were added to a glass cell fitted with a rubber septum until completely full. The protein was then added to get a final concentration between 20μM and 40μM (Hargrove 2000A). The wavelength monitored for Cgb Wt and the B10 mutants was 421nM.

Rapid Mixing

A BioLogic SFM 400 stopped-flow reactor connected with a MOS 250 spectrophometer was used to measure the rapid mixing of CO with protein. Solutions of CO or N_2 were prepared as performed in flash photolysis. Two syringes, one containing the deoxy ferrous protein and the other containing the desired concentration of CO, were used for mixing. The deoxy-ferrous form of the protein's spectrum was recorded first and compared to the CO bound protein's spectrum to check for the change in signal. Time courses were recorded with varying CO concentrations while observing the change in absorbance at 420nm. All data was collected at 20 °C (Smagghe et al 2006A).

CO Dissociation

CO dissociation experiments were preformed using a Varian Cary-Bio Spectrophotometer to measure the change in absorbance at 420nm over time all proteins except Rice Hb1, which was measured at 415nm. A cuvette was made ready by sealing with a rubber septum and flushing N_2 for five minutes. The NO solution was prepared by passing the NO through a 20% NaOH solution and bubbled into a 100mM potassium phosphate, pH 7.0, buffer for 20 minutes. One ml of the saturated NO solution was added to the cuvette and used as a blank. A few granules of dithionite were added to 20µl of a ~3mM concentrated protein solution followed by blowing CO over the protein solution for five minutes. About 2µl of protein solution was added to the NO solution and inverted three times before observing the changes in the spectrophotometer.

CO Equilibrium Titration

Saturated solutions of CO and N_2 were prepared as performed above in flash photolysis. CO equilibrium experiments were done using a Varian Cary-Bio Spectrophotometer to measure the change in absorbance at 420nm over all proteins except Rice Hb1, which was measured at 415nm. A cuvette was prepared by sealing with a rubber septum then flushing N_2 for five minutes. For Rice Hb1, about one ml, 995µl, of saturated N_2 solution was added to the cuvette and used to blank the spectrophotometer. Five µl of protein was added to the cuvette. CO was hand titrated into the cuvette and inverted three times followed by measuring the absorbance. This was done up to a concentration of 28µM CO and the absorption was corrected for the change in volume. Cgb Wt, Cgb B10A and Cgb B10F were examined similarly by hand titrating in CO till the solution in the cuvette reached a concentration of 10µM. The absorbance was not measured until 15 minutes after the addition of CO in insure that the mixture was in equilibrium. Additional cuvettes were prepared with initial concentrations of 950µM, 600µm, 200µm, 100µm, 30µM, 20uM and 15uM followed by the addition of the protein with absorbance measured after 15 minutes.

Electrochemistry

Potentiometric titrations were performed using the method described by Altuve et al 2004 with an Ocean-Optics UV-vis spectrophotometer (USB2000) and Oakton pH-mV meter (pH 1100 Series). A saturated calomel electrode (SCE) was used as a reference in combination with a platinum working electrode. Reduction potentials (E_{obs}) and mid-point potentials (E_{mid}) are reported with reference to a standard hydrogen electrode

(SHE). Titrations of ~30 µM Hb were carried out at 25°C in argon-saturated 0.1*M* potassium phosphate buffer, pH 7.0. Ferric proteins were titrated stepwise with a sodium dithionite solution (40 m*M*) previously sparged with argon. Reactions were monitored by recording the absorbance spectrum in the visible region (500-700 nm), and the corresponding cell potential (E_{obs}) was noted for each addition of dithionite solution after attainment of equilibrium.

A group of redox mediators were used to buffer the potential range from +160 to -440 mV. Their standard reduction potential *vs*. SHE are 1,2-naphthoquinone (E_{mid} = +157 mV), toluylene blue (E_{mid} = +115 mV), duroquinone (E_{mid} = +5 mV), hexaaminеruthenium(III) chloride (E_{mid} = +50 mV), pentaaminechlororuthenium(III) chloride (E_{mid} = -40 mV), 5,8-dihydroxy-1,4-naphthoquinone (E_{mid} = -50 mV), 2,5-dihydroxy-1-4-benzoquinone (E_{mid} = -60 mV), 2-hydroxy-1,4-naphthoquinone (E_{mid} = -137 mV), anthraquinone-1,5-disulfonic acid (E_{mid} = -175 mV), 9,10-anthraquinone-2,6-disulfonic acid (E_{mid} = -184 mV), and methyl viologen (E_{mid} = -440 mV) (Halder 2007).

Azide Equilibrium Titration

Azide equilibrium titration experiments were carried out using Varian Cary-Bio Spectrophotometer. Two solutions of sodium azide, 500mM and 5M, were prepared by dissolving sodium azide into 100mM potassium phosphate, pH 7.0, buffer. Cuvettes were made ready by adding ~1ml (995µl) of 100mM potassium phosphate, pH 7.0, buffer and used to blank the spectrophotometer. Five µl of concentrated protein solution was added and absorbance was measured at 415nm. For Cgb B10F the 500mM solution of sodium azide was hand titrated in 1µl at time using a 10µl Hamilton syringe until a

concentration of 5μM was reached in the cuvette and then the 5M sodium azide solution was added 1μl at time. Cgb Wt and Cgb B10A were hand titrated 1μl with the 5M sodium azide concentration. Absorbances at 415nm were measured 15 minutes after the addition of the sodium azide to allow it to reach equilibrium.

References

Adachi S., Sunohara N., Ishimori K. and Morishima I. Structure and Ligand Binding Properties of Leucine 29(B10) Mutants of Human Myoglobin. *JBC*. Vol. 267, 12614-21 (1992).

Altuve A., Wang L., Benson D. and Rivera M. Mammalian Mitochondrial and Microsomal Cytochromes b(5) Exhibit Divergent Structural and Biophysical Characteristics. *Biochem. Biophys. Res. Commun*. Vol. 314, 602-9 (2004).

Brucker E. A., Olson J. S., Phillips G. N. Jr., Dou Y. and Ikeda-Saito M. High Resolution Crystal Structure of the Deoxy, Oxy, and Aquomet forms of Cobalt Myoglobin. *JBC*. Vol. 271, 25419-22 (1996).

Carver T. E., Brantley R. E. Jr., Singleton E. W., Arduini R. M., Quillin, M. L., Phillips, G. N. Jr. and Olson, J. S. A Novel Site-directed Mutant of Myoglobin with an unusually high O2 Affinity and low Autooxidation Rate. *JBC*. Vol. 267, 6996-7010 (1992).

De Sanctis D., Dewilde S., Pesce A., Moens L., Ascenzi P., Hankeln T., Burmester T. and Bolognesi, M. Crystal Structure of Cytoglobin: The Fourth Globin Type Discovered in Man Displays Heme Hexa-Coordination. J.Mol.Biol. Vol. 336, 917 (2004).

Goodman M. D. and Hargrove M. S. Quaternary Structure of Rice Nonsymbiotic Hemoglobin. *JBC*. Vol. 276, 6834-39 (2001).

Halder P., Trent J. T. III & Hargrove M. S. Influence of the Protein Matrix on Intramolecular Histidine Ligation in Ferric and Ferrous Hexacoordinate Hemoglobins. *Proteins*. Vol. 66, 172-82 (2007).

Hargrove, M. S. A Flash Photolysis Method to Characterize Hexacoordinate Hemoglobin Kinetics. *Biophys. J*., Vol. 79, 631-51 (2000A).

Hargrove M. S., Brucker E. A., Stec B., Sarath G., Arredondo-Peter R., Klucas R. V., Olson J. S. and Phillips G. N. Jr. Crystal Structure of a Nonsymbiotic Plant Hemoglobin. *Structure*. Vol. 8, 1005-14 (2000B).

Kundu S., Trent J. T. III, & Hagrove M. S. Plants, Humans and Hemoglobins. *Trends Plant Sci.* Vol. 8, 387-93 (2003A).

Kundu S. and Hargrove M. S. Distal Heme Pocket Regulation of Ligand Binding and Stability in Soybean Leghemoglobin. *Proteins*. Vol. 50, 239-48 (2003B)

Kundu S., Blouin G. C., Premer S. A., Sarath G., Olson J. S. and Hargrove M. S. TryB10 Inhibits Stabilization of Bound Oxygen in Soybean Leghemoglobin. *Biochemistry*. Vol. 43, 6241-52 (2004).

Lassmann T. and Sonnhammer E. L. L. Kalign – An Accurate and Fast Multiple Sequence Alignment Algorithm. *BMC Bioinformatics*. Vol. 6, 298 (2005).

Perazzolli M., Dominici P., Romero-Puertas M., Zago E., Zeier J., Sonoda M., Lamb C. and Delledonne M. Arabidopsis Nonsymbiotic Hemoglobin AHb1 Modulates Nitric Oxide Bioactivity. Plant Cell. Vol. 10, 2785-94 (2004).

Olson J. S. Stopped-Flow, Rapid Mixing Measurements of ligand Binding to Hemoglobin and Red Cells. *Methods Enzymol*. Vol. 76, 631-51 (1981).

Smagghe B. J., Sarath G., Ross E., Hilbert J. & Hargrove M. S. Slow Ligand Binding Kinetics Dominate Ferrous Hexacoordinate Hemoglobin Reactivities and Reveal Differences between Plants and Other Species. *Biochemistry*, Vol. 45, 561-70 (2006A)

Smagghe B. J., Suman K., Hoy J. A., Halder P., Weiland T. R., Savage A., Venugopal A., Goodman M., Premer S., & Hargrove M. S. Role of Phenylalanine B10 in Plan Nonsymbiotic Hemoglobins. *Biochemistry*, Vol. 45, 9735-45 (2006B).

Trent J. T. III and Hargrove M. S. A Ubiquitously Expressed Human Hexacoordinate Hemoglobin. *JBC*. Vol. 277, 19538-45 (2002).

Wakasugi K., Nakano T., & Morishima I. Oxidized Human Neuroglobin Acts as a Heterotrimeric Gα Protein Guanine Nucleotide Dissociation Inihibotor. *JBC*, Vol. 278, No. 38 (2003).

Watts, R. Characterisation on Non-symbiotic Haemoglobins from Dicotyledonous Plants. *Doctoral Thesis*, Division of Biochemistry and Molecular Biology, Australian National University, Canberra, Australia (1999).

Wiltrout M. E., Giovannelli J. L., Simplaceanu V., Lukin J. A., Ho N. T. and Ho C. A Biophysical Investigation of Recombinant Hemoglobins with Aromatic B10 Mutations in the Distal Heme Pockets. *Biochemistry*. Vol. 44, 7207-17 (2005).